Vol. 78, No. 11

Murine Coronavirus Replication Induces Cell Cycle Arrest in G_0/G_1 Phase

Chun-Jen Chen† and Shinji Makino*

Department of Microbiology and Immunology, The University of Texas Medical Branch at Galveston, Galveston, Texas 77555-1019

Mouse hepatitis virus (MHV) replication in actively growing DBT and 17Cl-1 cells resulted in the inhibition of host cellular DNA synthesis and the accumulation of infected cells in the G_0/G_1 phase of the cell cycle. UV-irradiated MHV failed to inhibit host cellular DNA synthesis. MHV infection in quiescent 17Cl-1 cells that had been synchronized in the G_0 phase by serum deprivation prevented infected cells from entering the S phase after serum stimulation. MHV replication inhibited hyperphosphorylation of the retinoblastoma protein (pRb), the event that is necessary for cell cycle progression through late G_1 and into the S phase. While the amounts of the cellular cyclin-dependent kinase (Cdk) inhibitors $p21^{Cip1}$, $p27^{Kip1}$, and $p16^{INK4a}$ did not change in infected cells, MHV infection in asynchronous cultures induced a clear reduction in the amounts of Cdk4 and G_1 cyclins (cyclins D1, D2, D3, and E) in both DBT and 17Cl-1 cells and a reduction in Cdk6 levels in 17Cl-1 cells. Infection also resulted in a decrease in Cdk2 activity in both cell lines. MHV infection in quiescent 17Cl-1 cells prevented normal increases in Cdk4, Cdk6, cyclin D1, and cyclin D3 levels after serum stimulation. The amounts of cyclin D2 and cyclin E were not increased significantly after serum stimulation in mock-infected cells, whereas they were decreased in MHV-infected cells, suggesting the possibility that MHV infection may induce cyclin D2 and cyclin E degradation. Our data suggested that a reduction in the amounts of G_1 cyclin-Cdk complexes in MHV-infected cells led to a reduction in Cdk activities and insufficient hyperphosphorylation of pRb, resulting in inhibition of the cell cycle in the G_0/G_1 phase.

Many DNA viruses usurp host cell cycle regulation for their own replication advantage (reviewed in reference 56). Small DNA tumor viruses, such as simian virus 40 (13, 22), adenovirus (18, 36), and human papillomavirus (75, 79), encode proteins that promote cells to enter the S phase. In contrast, herpesviruses, a group of large DNA viruses that encode their own DNA polymerases, generally block cell cycle progression at the G_0/G_1 phase during lytic infection cycles (reviewed in reference 25). Studies of cell cycle dysregulation induced by RNA viruses have been relatively limited. That reovirus infection causes the inhibition of cellular DNA synthesis has been known for some time (12, 20, 30), but not until more recently was it shown that reovirus-induced inhibition of cell proliferation results from G_2/M cell cycle arrest that is mediated by the viral σ1s nonstructural protein (59). Human immunodeficiency virus type 1 infection also induces cell cycle arrest in the G_2/M phase (32), and the expression of the accessory gene product Vpr alone is sufficient for inducing G_2/M cell cycle arrest (60, 62). Vpr-mediated cell cycle arrest apparently favors virus replication, since the long terminal repeat is most active and the expression of the viral genome is optimal in the G_2 phase of the cell cycle (27). Cell cycle perturbations have also been seen in cells infected with the paramyxovirus simian virus 5 (44), measles virus (49, 50, 53), and coxsackievirus (48).

Cyclins and cyclin-dependent kinases (Cdks) form complexes and play important regulatory roles in controlling cell cycle progression (reviewed in references 55 and 58). G_1-phase progression requires the activities of cyclin D-Cdk4/6 complexes, and cyclin E-Cdk2 activity is necessary for the G_1/S-phase transition. These G_1 cyclin-Cdk complexes regulate the cell cycle through phosphorylation of the retinoblastoma protein (pRb) p107 and pRB family proteins and p130. In the quiescent G_0 phase, pRb is nonphosphorylated, while during the G_1 phase, it is sequentially hypophosphorylated by cyclin D-Cdk4/6 complexes in early G_1 and hyperphosphorylated by the cyclin E-Cdk2 complex in late G_1 (47). It remains hyperphosphorylated in the S, G_2, and M phases of cycling cells (14). When pRb binds to the E2F family of transcription factors, it functions as a transcriptional repressor, and its hyperphosphorylation in late G_1 results in inactivation, release of E2F, and transcription of genes important for DNA synthesis (reviewed in references 17 and 31).

The activities of G_1 cyclin-Cdk complexes are regulated by cellular Cdk inhibitors (CKIs) (reviewed in reference 65). INK4 family CKIs bind to Cdk4 and Cdk6, thus blocking cyclin D-Cdk4/6 activities (reviewed in references 63 and 64). CKIs of the Cip/Kip family, including $p21^{Cip1}$, $p27^{Kip1}$, and $p57^{Kip2}$, are potent inhibitors of cyclin E- and A-dependent Cdk2 (reviewed in reference 51). The regulation of G_1 cyclin quantities is also important for proper cell cycle progression. Cyclin D1 expression is induced through the RAS-RAF-MEK-ERK pathway upon mitogenic stimulation (1, 24, 38, 43, 77), and cyclin D1 undergoes ubiquitin-dependent proteolysis when it is phosphorylated by glycogen synthase kinase 3β (15). The presence of growth factors maintains D-type cyclins at relatively constant levels throughout the cell cycle. The amounts of cyclin E

* Corresponding author. Mailing address: Department of Microbiology and Immunology, The University of Texas Medical Branch at Galveston, MRB 4.146, 301 University Blvd., Galveston, TX 77555-1019. Phone: (409) 772-2323. Fax: (409) 772-5065. E-mail: shmakino @utmb.edu.
† Present address: Department of Pathology, University of Massachusetts Medical School, Worcester, MA 01655.

in actively growing cells are maximal at the G_1/S-phase transition and low in other cell cycle phases (6, 26). The synthesis of cyclin E occurs in the late G_1 phase and is transcriptionally controlled by E2F transcription factors. Rapid turnover of cyclin E in the S phase is mediated by phosphorylation-dependent ubiquitination and subsequent proteolysis (9, 52, 80).

Coronaviruses are enveloped RNA viruses that cause gastrointestinal and upper respiratory tract illnesses in animals and humans (57, 78). Recently, a novel coronavirus was shown to be the etiologic agent for the emerging infectious disease severe acute respiratory syndrome (16, 42). Mouse hepatitis virus (MHV), a prototypic coronavirus, causes various diseases, including hepatitis, enteritis, and encephalitis, in rodents (10, 78). After MHV infection, MHV RNA synthesis takes place in the cytoplasm. MHV particles, which contain three envelope proteins, S, M, and E, and an internal helical nucleocapsid, which consists of N protein and genomic RNA, bud from internal cellular membranes (40, 45, 74). Extensive morphological, physiological, and biological changes occur in cells infected with MHV (2, 3, 33, 66, 70, 71), and MHV infection may induce apoptotic cell death in certain cultured cell lines at a time late in infection (2, 4, 7).

Knowledge of how coronavirus infection may affect host cell cycle regulation is still limited. The expression of N protein of infectious bronchitis virus (IBV), an avian coronavirus, causes delayed cell growth (8). Furthermore, cells expressing transmissible gastroenteritis virus N protein or IBV N protein, as well as cells infected with IBV, exhibit aberrant cell division, indicating that cytokinesis is disrupted (8, 81). Whether MHV infection or MHV N protein expression has similar effects on cell growth and cytokinesis is unknown.

In the present study, we examined the effect of MHV replication on cell cycle progression. We found that MHV infection in asynchronously growing cells led to the inhibition of host DNA synthesis and the accumulation of infected cells in the G_0/G_1 phase. When serum-starved, quiescent cells were infected with MHV, they failed to enter the S phase after serum stimulation. Further analyses suggested that a reduction in the amounts of Cdk4, Cdk6, and G_1 cyclins in infected cells resulted in the accumulation of hypophosphorylated and/or nonphosphorylated pRb, leading to the arrest of cell cycle progression in the G_0/G_1 phase.

MATERIALS AND METHODS

Virus and cells. Plaque-cloned MHV type 2 (MHV-2) was used throughout this study. Mouse fibroblast 17Cl-1 cells (69) and astrocytoma DBT cells (34) were maintained as previously described (7).

Cell cycle analysis by flow cytometry. Nuclear DNA content was measured by using propidium iodide staining and fluorescence-activated cell sorting (FACS) analysis as described previously (82). Briefly, adherent cells were treated with trypsin, washed with phosphate-buffered saline (PBS), resuspended in low-salt stain buffer (3% polyethylene glycol 8000, 50 μg of propidium iodide/ml, 0.1% Triton X-100, 4 mM sodium citrate, 10 μg of RNase A/ml), and incubated at 37°C for 20 min. An equal volume of high-salt stain buffer (3% polyethylene glycol 8000, 50 μg of propidium iodide/ml, 0.1% Triton X-100, 400 mM sodium chloride) then was added to the cell suspension. Propidium iodide-stained nuclei were stored at 4°C overnight before FACS analysis (FACScan; Becton Dickinson), and at least 15,000 nuclei were counted for each sample. Data analysis was performed by using ModFit LT version 2.0 (Verity Software House).

Measurement of cellular DNA synthesis. 17Cl-1 cells or DBT cells plated in 96-well plates at approximately 50% confluence were mock infected or infected with MHV-2 at a multiplicity of infection (MOI) of 20. Cells were labeled continuously with 1 μCi of [³H]thymidine (Amersham)/well from 4 to 11 h

postinfection (p.i.) and harvested onto glass fiber filters (Packard) with a cell harvester (Packard). Total [³H]thymidine incorporation into the cells was determined by scintillation counting (Beckman LS 6000IC).

Synchronization of cells. Subconfluent cultures of 17Cl-1 cells were synchronized in the G_0 phase by using serum deprivation. Approximately 4×10^5 cells were plated in a 60-mm plate and maintained in medium containing 0.5% fetal calf serum (FCS) for 48 h. Synchronized cells were mock infected or infected with MHV-2 at an MOI of 10. After 1 h of virus adsorption, cells were treated with medium containing 10% FCS and harvested at various times p.i. for cell cycle and Western blot analyses.

Total cell lysate preparation. Infected and mock-infected cells were collected at various times after MHV-2 inoculation and washed once with PBS. Cells were lysed directly in sodium dodecyl sulfate (SDS) sample buffer (60 mM Tris-HCl [pH 6.8], 2% SDS, 10% glycerol, 5% 2-mercaptoethanol, 0.01% bromophenol blue), boiled for 10 min, and passed through a 23-gauge needle several times to shear the DNA.

Western blot analysis. Whole-cell lysates separated by SDS-polyacrylamide gel electrophoresis were transferred to polyvinylidene difluoride membranes (Amersham). The membranes were blocked in blocking solution (0.05% Tween 20 and 5% nonfat dry milk in PBS), incubated with primary and secondary antibodies diluted in blocking solution for 1 h each, and developed with an enhanced chemiluminescence kit (Amersham). The following mouse monoclonal antibodies were used: anti-pRb (G3-245; BD Pharmingen); anti-cyclin D1 (Ab-3; Oncogene); and anti-Cdk2, anti-Cdk4, and anti-cyclin D3 (BD Biosciences). The following rabbit polyclonal antibodies were used: anti-p21 (C-19), anti-cyclin E (M-20), anti-Cdk6 (C-21), anti-cyclin D2 (M-20), and anti-p16 (M-156) (Santa Cruz Biotechnology); anti-p27 (2552; Cell Signaling); and anti-phospho-pRb (Ser807 and Ser811) (9308; Cell Signaling). Actin was detected with goat anti-actin polyclonal antibody (I-19; Santa Cruz Biotechnology). Horseradish peroxidase-conjugated goat anti-mouse and anti-rabbit immunoglobulin G antibodies and donkey anti-goat immunoglobulin G antibody (Santa Cruz Biotechnology) were used as secondary antibodies.

Cdk2 kinase assay. Cells were lysed in lysis-immunoprecipitation buffer (50 mM Tris-HCl [pH 7.5], 150 mM NaCl, 0.5% NP-40, 50 mM NaF, 1 mM dithiothreitol, 1 mM phenylmethylsulfonyl fluoride, protease inhibitor cocktail [P8340; Sigma], phosphatase inhibitor cocktails [P2850 and P5726; Sigma]). Five hundred micrograms of protein lysate from each sample was immunoprecipitated with 2 μg of anti-Cdk2 antibody (M-2; Santa Cruz Biotechnology) and protein A beads. The immunocomplexes were washed twice with lysis-immunoprecipitation buffer and twice with kinase buffer (25 mM Tris-HCl [pH 7.5], 5 mM β-glycerophosphate, 2 mM dithiothreitol, 0.1 mM Na_3VO_4, 10 mM $MgCl_2$; Cell Signaling) and then incubated in kinase buffer containing 200 μM ATP and 1 μg of a fusion protein containing maltose binding protein and the C-terminal region (701 to 928) of pRb (Rb-C) (Cell Signaling) at 30°C for 30 min. The reaction was stopped by adding SDS sample buffer and boiling the samples for 5 min. Proteins were separated on SDS–8% polyacrylamide gels and visualized by Western blot analysis with an anti-phospho-pRb (Ser807 and Ser811) antibody.

Statistical and densitometric analyses. Statistical analysis was performed by using Student's t test. Data are reported as the mean and standard error (SE). A P value of <0.05 was considered significant. Bands on Western blots were scanned, and the mean density of each band was analyzed by using *Total*Lab software (Ultra · Lum Inc., Claremont, Calif.); prior titration experiments had confirmed that image densities were linearly proportional to protein masses. Each protein signal was normalized against the actin signal in each sample before comparisons for fold changes.

RESULTS

Most MHV laboratory strains cause prominent cell fusion in infected cell cultures, whereas cells infected with MHV-2 do not show syncytium formation; only a rounding-type cytopathic effect can be seen at late stages of MHV-2 infection (34, 37). It is unlikely that the cell cycle could progress properly in fused cells; therefore, we chose to use exclusively MHV-2 to study the effect of MHV replication on cell cycle progression.

MHV replication inhibits cell proliferation and cellular DNA synthesis. Over the course of our day-to-day routine, we noticed that when subconfluent 17Cl-1 or DBT cell cultures were infected with MHV-2, the cultures remained at that subconfluent level throughout infection; simultaneously, however,
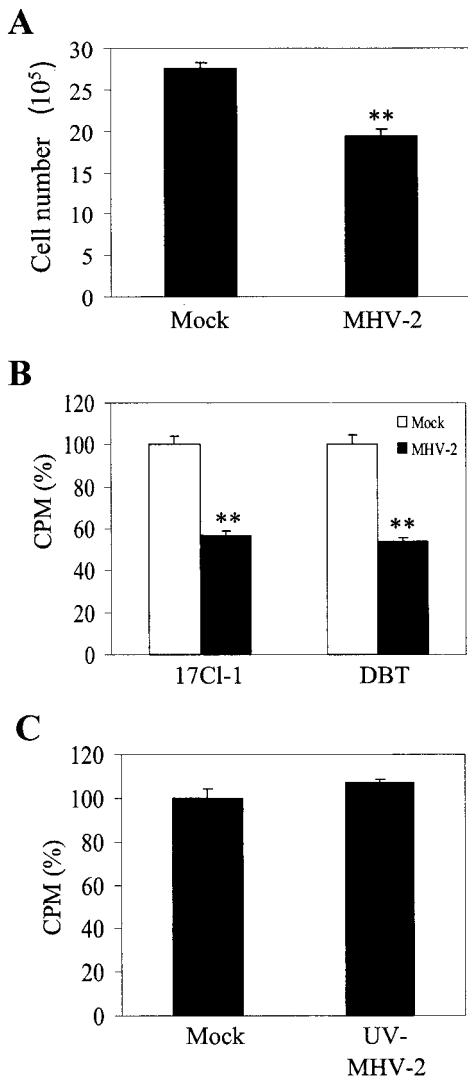
FIG. 1. MHV infection inhibits cell proliferation and cellular DNA synthesis. (A) 17Cl-1 cells at 30% confluence in a 6-cm dish were mock infected or infected with MHV-2 at an MOI of 10. At 18 h p.i., cell numbers were counted in a hemocytometer. The data are presented as means and SEs ($n = 5$). (B) 17Cl-1 cells and DBT cells were mock infected or infected with MHV-2 at an MOI of 20. Cellular DNA synthesis was measured by [³H]thymidine incorporation from 4 to 11 h p.i. The results are presented as the mean and SE counts per minute (CPM) for six independent experiments. The CPM for MHV-infected samples were normalized to the CPM for mock-infected samples (100%). (C) 17Cl-1 cells were mock infected or infected with UV-inactivated MHV-2, and cellular DNA synthesis was measured as described for panel B. Double asterisks indicate a P value of < 0.001 in comparisons with mock-infected samples.

the same cultures treated as mock-infected controls reached confluence. The observed dissimilarity in cell confluence between mock-infected and infected cultures led us to speculate that MHV-2 infection inhibited cell proliferation. Figure 1A shows that at 18 h p.i., an MHV-infected 17Cl-1 cell culture had a significantly smaller number of cells than did a mock-infected cell culture. This smaller number of cells in the MHV-infected culture was not due to cell death, as >98% of MHV-infected 17Cl-1 cells excluded trypan blue stain at 18 h p.i. We

further examined the effect of MHV infection on cellular DNA synthesis by measuring [³H]thymidine incorporation into MHV-infected cells and mock-infected cells. DBT cells and 17Cl-1 cells, both of which were about 50% confluent, were infected with MHV or mock infected and then labeled with [³H]thymidine from 4 to11 h p.i. Analysis of radioisotope incorporation into host DNA showed significant reductions in the incorporation of [³H]thymidine into MHV-infected cells compared with mock-infected control cells for both cell lines (Fig. 1B), demonstrating that host DNA synthesis was inhibited in MHV-infected cells and that this effect was not cell type specific.

To test whether the binding of MHV to MHV receptors or some unidentified substances present in the inoculum caused the inhibition of cellular DNA synthesis, MHV was inactivated by irradiation of the inoculum with UV light prior to addition to 17Cl-1 cells, and [³H]thymidine incorporation was measured as described above. There was no significant difference in [³H]thymidine uptake between mock-infected cells and cells treated with UV-inactivated MHV (Fig. 1C), demonstrating that the binding of MHV to MHV receptors alone or unidentified substances present in the inoculum did not affect host DNA synthesis. The replication of MHV was necessary to induce the inhibition of cellular DNA synthesis.

MHV-infected cells accumulate in the G_0/G_1 phase of the cell cycle. We next monitored cell cycle profiles of mock-infected and MHV-infected cells to determine whether the inhibition of cellular DNA synthesis in infected cells was due to a perturbation in cell cycle progression, particularly S-phase entry. Asynchronously growing DBT and 17Cl-1 cell cultures at about 50% confluence were mock infected or infected with MHV. Cells were harvested at various times p.i., and nuclear DNA was stained with propidium iodide prior to FACS analysis for the measurement of DNA content (Fig. 2A). The histograms were further analyzed quantitatively by a curve-fitting program to determine the percentage of cells in each of the G_0/G_1, S, and G_2/M phases (Fig. 2B); G_0/G_1-phase cells showed 2N DNA content, and G_2/M-phase cells showed 4N DNA content. For both cell lines, slightly higher percentages of MHV-infected cells than of mock-infected cells were in the G_0/G_1 phase at 4 and 8 h p.i. This trend was further enhanced at 12 h p.i., at which time nearly 10 and 20% larger G_0/G_1-phase populations were present in MHV-infected cells than in mock-infected cells for the DBT and the 17Cl-1 cell lines, respectively (Fig. 2B). These data strongly suggested that MHV infection resulted in the arrest of the cell cycle in the G_0/G_1 phase and that prevention of infected cells from entering the S phase caused the inhibition of cellular DNA synthesis. The number of nuclei with subdiploidic DNA content was almost negligible in all MHV-infected DBT and 17Cl-1 cell samples (Fig. 2A), demonstrating that infected cells did not undergo apoptotic cell death before 12 h p.i.

MHV infection of quiescent cells prevents cell cycle reentry. To further establish that MHV replication caused G_0/G_1 cell cycle arrest, we infected serum-starved quiescent cells with MHV and examined cell cycle progression after serum stimulation. Synchronization of 17Cl-1 cells in the quiescent state could be achieved by culturing cells in a medium containing 0.5% FCS for 48 h, whereas we were unable to synchronize DBT cells by serum deprivation. Quiescent 17Cl-1 cells at

A

B
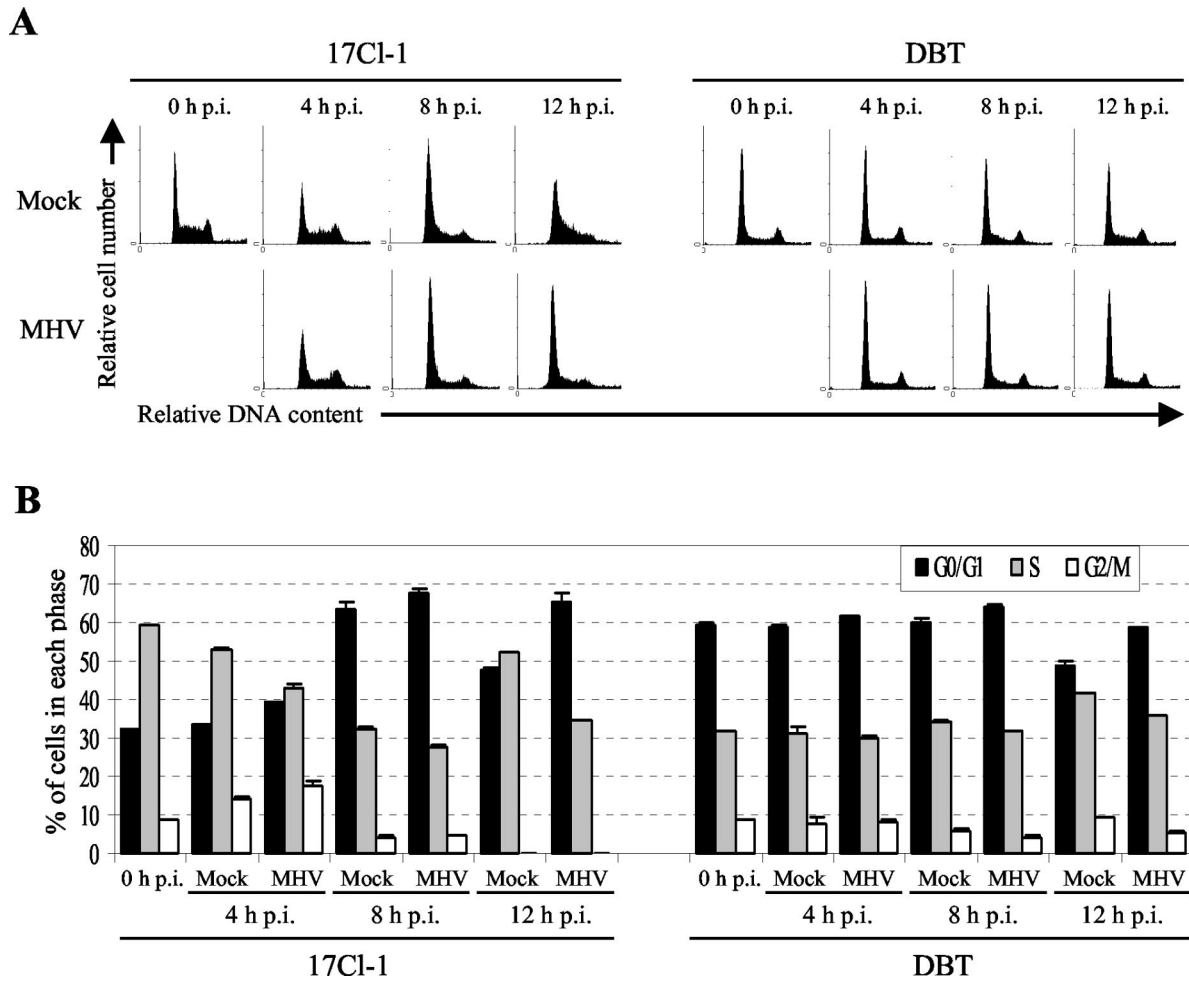
FIG. 2. MHV infection in asynchronously growing cells induces the accumulation of cells in the G_0/G_1 phase of the cell cycle. (A) DBT and 17Cl-1 cells were mock infected (Mock) or infected with MHV-2 (MHV) at an MOI of 10. At the indicated times p.i., cells were collected and stained with propidium iodide for FACS analysis. The data are from one of three experiments. (B) The histograms in panel A were analyzed by the ModFit LT program to determine the percentage of cells in each phase of the cell cycle. The results are presented as means and SEs for three experiments. The S- and G_2/M-phase populations in mock- and MHV-infected 17Cl-1 cells at 12 h p.i. were combined and presented as the S-phase population because the G_2/M-phase population in these histograms could not be identified accurately by the ModFit LT program.

about 50% confluence were infected with MHV or mock infected. After virus adsorption for 1 h, both mock-infected and MHV-infected cells were incubated in a medium containing 10% FCS to provide mitogenic stimuli for cell cycle reentry. Our preliminary experiments showed that quiescent 17Cl-1 cells started to enter the S phase at about 12 h after serum stimulation (data not shown); therefore, we examined the effect of MHV infection on cell cycle progression at various times only after 12 h of serum stimulation. Figure 3A shows histograms of DNA content determined by FACS analysis, and the quantitative results are shown in Fig. 3B. Prior to infection, about 70% of serum-starved cells were arrested in the G_0/G_1 phase. At 15 h p.i., mock-infected cells showed a decrease in the G_0/G_1-phase population and an increase in the S-phase population, and this trend was further enhanced at 18 h p.i.; these results indicated that quiescent 17Cl-1 cells reentered the cell cycle after serum stimulation. Quite the opposite was true for the majority of MHV-infected cells, which remained in the G_0/G_1 phase at 15 and 18 h p.i.; these results demonstrated

that infected cells were unable to progress from the G_0/G_1 phase to the S phase and were consistent with the above observations that asynchronous cultures accumulated in the G_0/G_1 phase after MHV infection (Fig. 2). These data suggested that MHV replication arrested cell cycle progression in the G_0/G_1 phase.

MHV infection causes a change in the phosphorylation status of pRb. One key regulator of cell cycle progression from the G_0/G_1 phase to the S phase is pRb, which binds to E2F transcription factors and inhibits their activities. In the late G_1 phase, hyperphosphorylation of pRb by cyclin E-Cdk2 allows the release and activation of E2F, which then promotes progression to the S phase. To understand the mechanism of MHV-induced G_0/G_1 cell cycle arrest, we first examined the pRb phosphorylation status in MHV-infected cells. Asynchronously growing DBT and 17Cl-1 cells at about 50% confluence were infected with MHV or mock infected, and whole-cell lysates were prepared at 0, 4, 8, and 12 h p.i. The phosphorylation status of pRb was determined by Western blot analysis

A

B
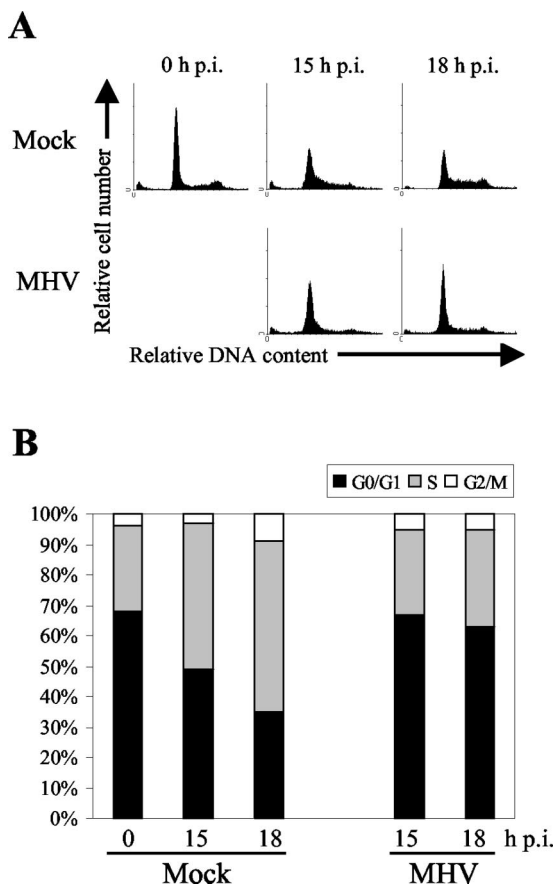
FIG. 3. MHV infection of quiescent 17Cl-1 cells prevents cell cycle reentry. (A) Serum-starved 17Cl-1 cells were mock infected (Mock) or infected with MHV-2 (MHV) at an MOI of 10. After 1 h of virus adsorption, medium containing 10% FCS was added to the cells, and cell cycle profiles at the indicated times p.i. were determined by FACS analysis. The data are from one of three experiments. (B) The histograms in panel A were analyzed by the Synch Wizard algorithm of the ModFit LT program to determine the percentage of cells in each phase of the cell cycle.

with an anti-pRb monoclonal antibody that recognizes the nonphosphorylated form and all of the phosphorylated forms of pRb; in bisacrylamide cross-linked gels, hyperphosphorylated pRb migrates slowly, while hypophosphorylated and nonphosphorylated forms of pRb comigrate and appear as a rapidly migrating band (21). In mock-infected DBT (Fig. 4A) and 17Cl-1 (Fig. 4B) cells, the majority of pRb appeared as a slowly migrating, hyperphosphorylated form at any given time p.i., indicating that most of the cells were actively progressing through the cell cycle. The results were markedly different with MHV infection; in both cell lines, MHV infection resulted in the accumulation of nonphosphorylated and/or hypophosphorylated pRb, which was particularly prominent in infected 17Cl-1 cells at 8 and 12 h p.i. (Fig. 4B, lanes 5 and 7). These data demonstrated the inhibition of pRb hyperphosphorylation in MHV-infected cells. Hyperphosphorylation of pRb occurs in the late G_1 phase, and hyperphosphorylated pRb is not dephosphorylated until cells complete mitosis and reenter the G_1 phase (reviewed in reference 72). Therefore, the accumulation of nonphosphorylated and/or hypophosphorylated pRb

A

B

C
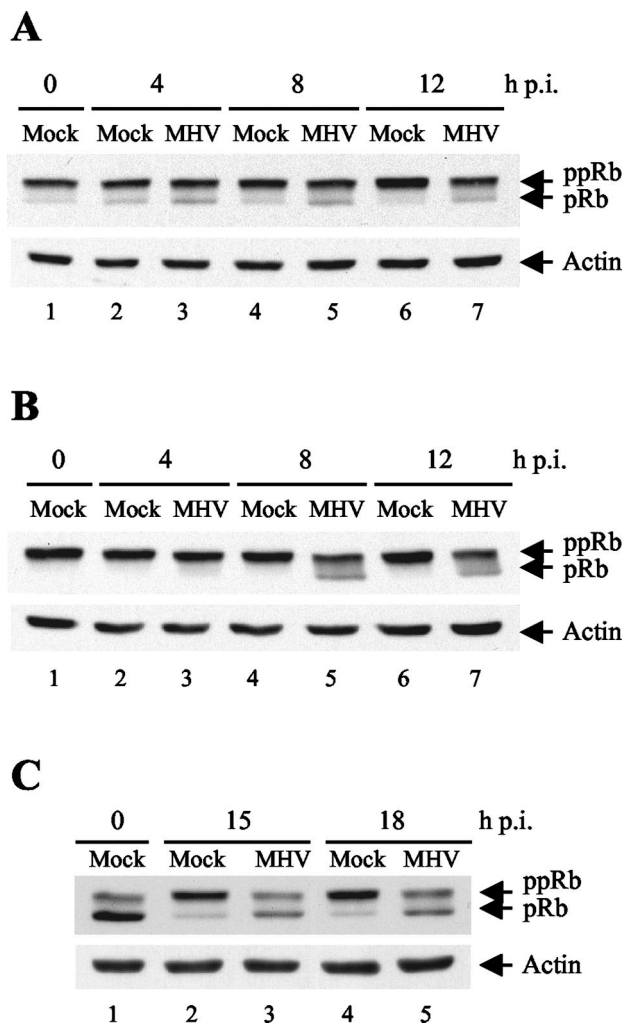
FIG. 4. MHV infection induces the accumulation of nonphosphorylated and/or hypophosphorylated pRb. Asynchronously growing DBT cells (A) and 17Cl-1 cells (B) were mock infected (Mock) or infected with MHV-2 (MHV) at an MOI of 10. At the indicated times p.i., cells were lysed with SDS sample buffer, and equal amounts of protein from the samples were subjected to Western blot analysis for pRb and actin. Nonphosphorylated and hypophosphorylated forms of pRb (pRb) appeared as rapidly migrating bands, and hyperphosphorylated pRb (ppRb) appeared as slowly migrating bands. (C) Serum-starved 17Cl-1 cells were mock infected (Mock) or infected with MHV-2 (MHV) at an MOI of 10. After 1 h of virus adsorption, medium containing 10% FCS was added to the cells. At the indicated times p.i., cell lysates were collected and analyzed as described above. Similar results were obtained in three independent experiments.

in MHV-infected cells suggested that once pRb was dephosphorylated at the completion of mitosis, it could not be hyperphosphorylated again by cyclin E-Cdk2. As a result, MHV infection might trigger cell cycle arrest in the early G_1 phase.

We next examined how MHV infection affected pRb phosphorylation when quiescent 17Cl-1 cells were released from G_0 arrest and allowed to reenter the cell cycle. Subconfluent 17Cl-1 cells were synchronized by serum deprivation as described earlier. After virus adsorption for 1 h, MHV-infected and mock-infected cells were stimulated with 10% FCS, and the phosphorylation status of pRb at different times p.i. was

A

B
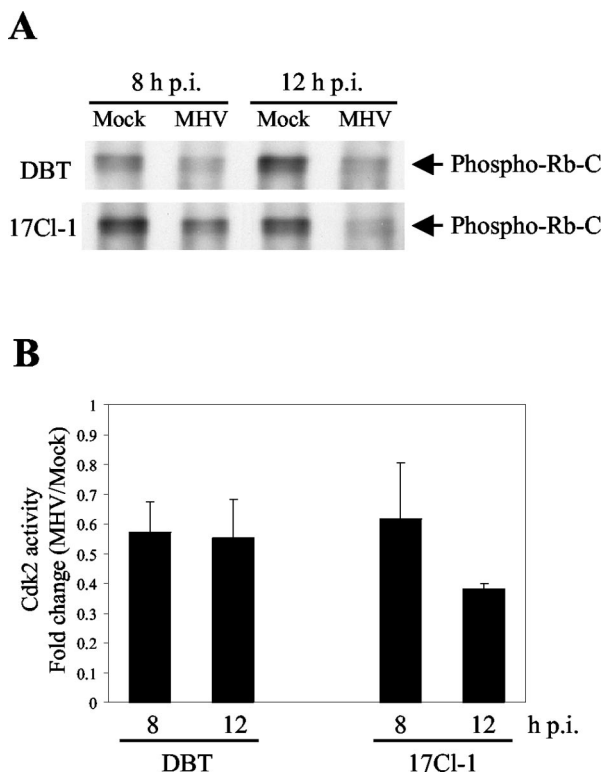
FIG. 5. Effect of MHV infection on Cdk2 activity. (A) Cdk2 was immunoprecipitated from mock-infected (Mock) or MHV-2-infected (MHV) DBT and 17Cl-1 cell lysates, and kinase activities were determined by an immunocomplex kinase assay with Rb-C as a substrate followed by Western blot analysis for Rb-C phosphorylation at Ser807 and Ser811 (phospho-Rb-C). The data are from one of three independent experiments. (B) Cdk2 activities in panel A were quantified by densitometric analysis, and the ratio of activity in MHV-infected samples to that in mock-infected samples is presented as the mean and SE ($n = 3$).

determined by Western blot analysis. In serum-starved 17Cl-1 cells that were synchronized in the G_0 phase, pRb appeared in the gel primarily as a rapidly migrating band (Fig. 4C, lane 1) consisting mostly of nonphosphorylated pRb. After mitogenic stimulation, the majority of pRb was converted to the hyperphosphorylated form in mock-infected cells at 15 and 18 h p.i.

(Fig. 4C, lanes 2 and 4), consistent with the data in Fig. 3 showing that uninfected cells could progress from the G_0 phase to the S phase after serum stimulation. In contrast, the accumulation of hyperphosphorylated pRb did not occur in MHV-infected cells at 15 and 18 h p.i. (Fig. 4C, lanes 3 and 5). These data corroborated the FACS analysis data; MHV infection inhibited the cell cycle reentry of quiescent cells after serum stimulation (Fig. 3). Altogether, our results indicated that MHV infection induced the accumulation of nonphosphorylated and/or hypophosphorylated pRb, which in turn suppressed E2F activity and S-phase entry, leading to the accumulation of cells in the G_0/G_1 phase of the cell cycle.

Effect of MHV infection on Cdk2 activity. G_1 cyclin-Cdk complexes regulate cell cycle progression through the phosphorylation of pRb. Accordingly, the inhibition of pRb hyperphosphorylation in MHV-infected cells suggested that the functions of G_1 cyclin-Cdk complexes were suppressed. To verify this possibility, we tested how MHV infection affected Cdk2 activity, which regulates pRb hyperphosphorylation and progression from the G_1 phase to the S phase. Cdk2 activity was analyzed by means of an in vitro kinase assay with an Rb-C fusion protein as a substrate. This substrate fusion protein contains maltose binding protein the C-terminal region (701 to 928) of pRb, which can be phosphorylated by various cyclin-Cdk complexes (11, 39, 41). Because pRb residues Ser807 and Ser811 are preferentially phosphorylated by cyclin E-Cdk2 or cyclin A-Cdk2 (11), we measured Cdk2 activity by detecting Ser807- and Ser811-specific phosphorylation of Rb-C by Western blot analysis (Fig. 5A). Figure 5B shows quantitative data from the scanning densitometric analysis. For both DBT and 17Cl-1 cells, there was a significant reduction in Cdk2 activity in MHV-infected cells compared with mock-infected cells at 8 and 12 h p.i., consistent with the previous data showing that pRb hyperphosphorylation was suppressed in MHV-infected cells (Fig. 4). We attempted to measure Cdk4 activity, but we could not successfully establish an in vitro Cdk4 kinase assay by measuring Cdk4-specific phosphorylation of Rb-C at Ser780 (39) (data not shown).

Quantitative analyses of CKIs, cyclins, and Cdks in infected cells. Because the activities of G_1 cyclin-Cdk complexes are regulated by Cip/Kip family and INK4 family CKIs (reviewed in reference 65), we explored the possibility that MHV repli-
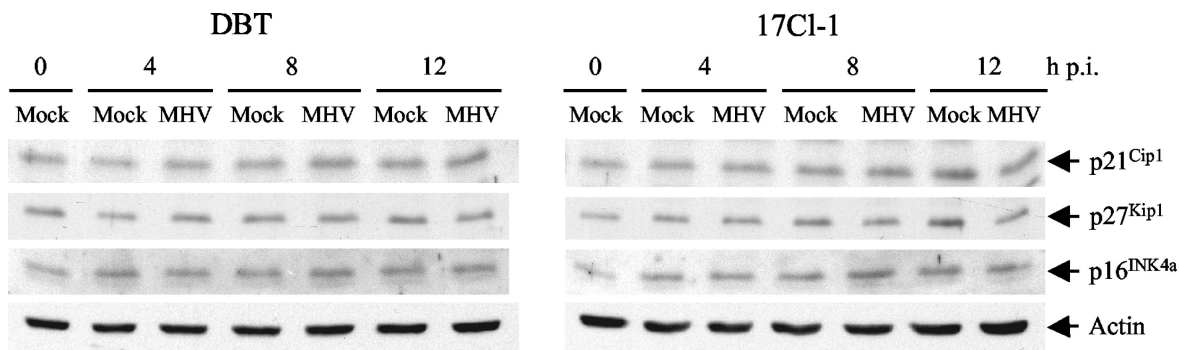
FIG. 6. Effect of MHV infection on the levels of expression of the cellular CKIs p21[Cip1], p27[Kip1], and p16[INK4a]. Asynchronously growing DBT cells and 17Cl-1 cells were mock infected (Mock) or infected with MHV-2 (MHV) at an MOI of 10. At the indicated times p.i., cells were lysed with SDS sample buffer, and equal amounts of protein from the samples were tested by Western blot analysis against probes for p21[Cip1], p27[Kip1], p16[INK4a], and actin. The data are from one of three independent experiments.

A

B
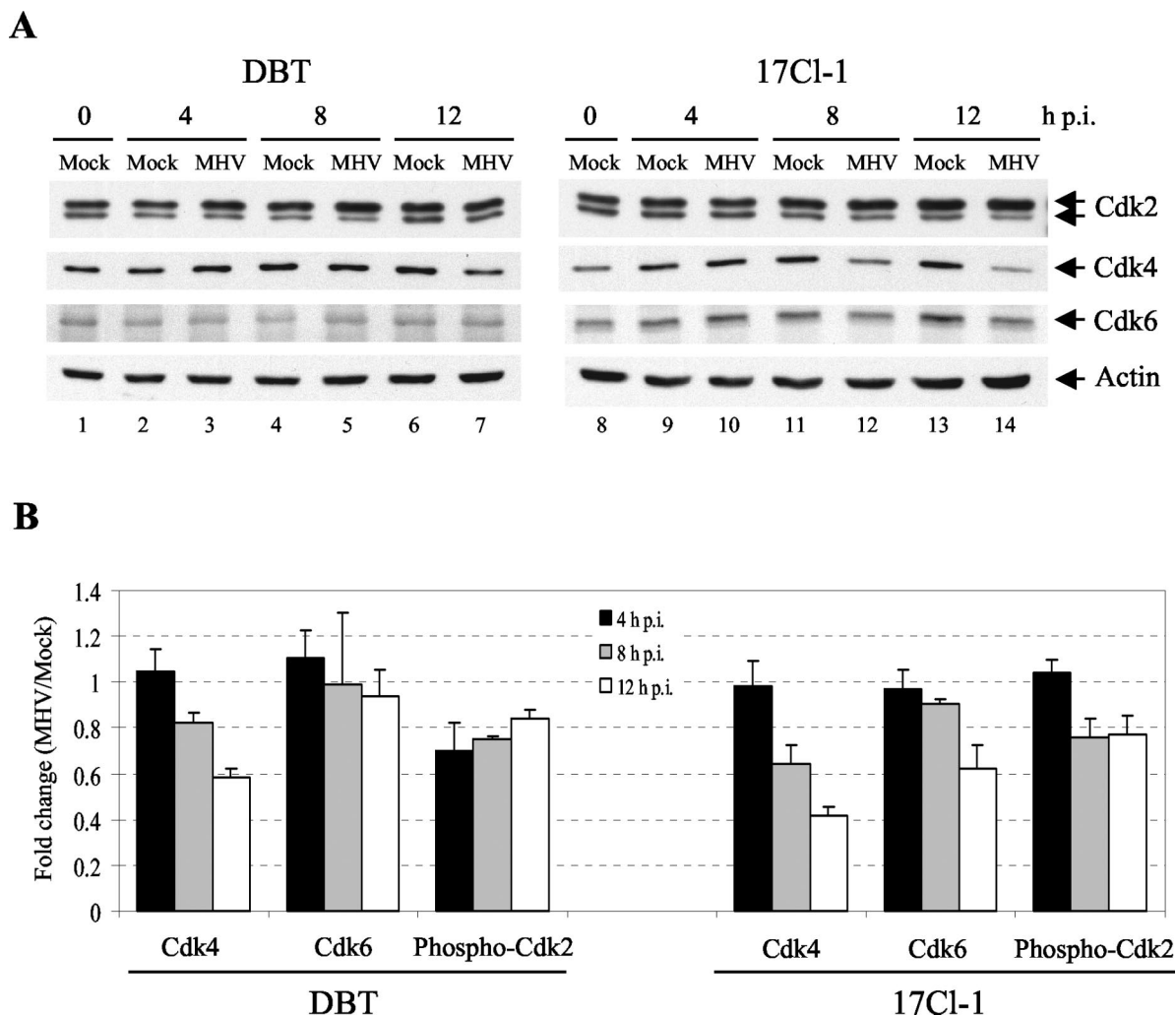
FIG. 7. Effect of MHV infection on levels of G_1 Cdks in asynchronously growing cells. (A) DBT and 17Cl-1 cells were mock infected (Mock) or infected with MHV-2 (MHV) at an MOI of 10. At the indicated times p.i., cells were lysed with SDS sample buffer, and equal amounts of protein from the samples were tested by Western blot analysis against probes for Cdk2, Cdk4, Cdk6, and actin. The data are from one of three independent experiments. (B) Cdk amounts in panel A were quantified by densitometric analysis and normalized against an internal control (actin). Bars indicate the ratio of Cdk amounts in MHV-infected samples to those in mock-infected samples. The results are presented as means and SEs (n = 3).

cation induces the accumulation of CKIs, including p21[Cip1], p27[Kip1], and p16[INK4a]. DBT and 17Cl-1 cells at about 50% confluence were mock infected or infected with MHV. Total cell lysates were prepared at 0, 4, 8, and 12 h p.i., and the amounts of p21[Cip1], p27[Kip1], and p16[INK4a] were determined by Western blot analysis (Fig. 6). For both cell lines examined, there was no significant difference in the amounts of these CKIs between mock-infected and MHV-infected cells at any given time p.i., indicating that MHV-induced G_0/G_1 cell cycle arrest did not involve the activation of p21[Cip1], p27[Kip1], and p16[INK4a].

If the amounts of G_1 cyclin-Cdk complexes are low in MHV-infected cells, then pRb hyperphosphorylation is likely to be inhibited. To explore this possibility, we measured the levels of Cdk2, Cdk4, and Cdk6 (Fig. 7A) and of cyclins D1, D2, D3, and E (Fig. 8A) in MHV-infected and mock-infected cells by Western blot analysis. As described by others (23, 61), Cdk2

appeared in the gel as two discrete bands, the rapidly migrating, phosphorylated band and the slowly migrating, nonphosphorylated band (Fig. 7A). Cdk2 phosphorylation, which is mediated by the Cdk-activating kinase, is required for full activation of the cyclin E-Cdk2 complex (23, 29). The anti-cyclin D2 antibody detected both cyclins D1 and D2 due to its cross-reactivity (Fig. 8A). In the scanning densitometric analysis, each protein signal was normalized against the actin signal in the same sample as an internal control, and then the fold change in the level of each protein between MHV-infected and mock-infected samples at each time was calculated (Fig. 7B and 8B). For both DBT and 17Cl-1 cells, MHV-infected cells had smaller amounts of Cdk4 than did mock-infected cells at 8 and 12 h p.i. (Fig. 7). MHV-infected 17Cl-1 cells also exhibited decreases in Cdk6 and phospho-Cdk2 levels at later times p.i., while these changes were less prominent in MHV-infected DBT cells. For G_1 cyclins, the amounts of cyclins D1, D2, D3,

A

B
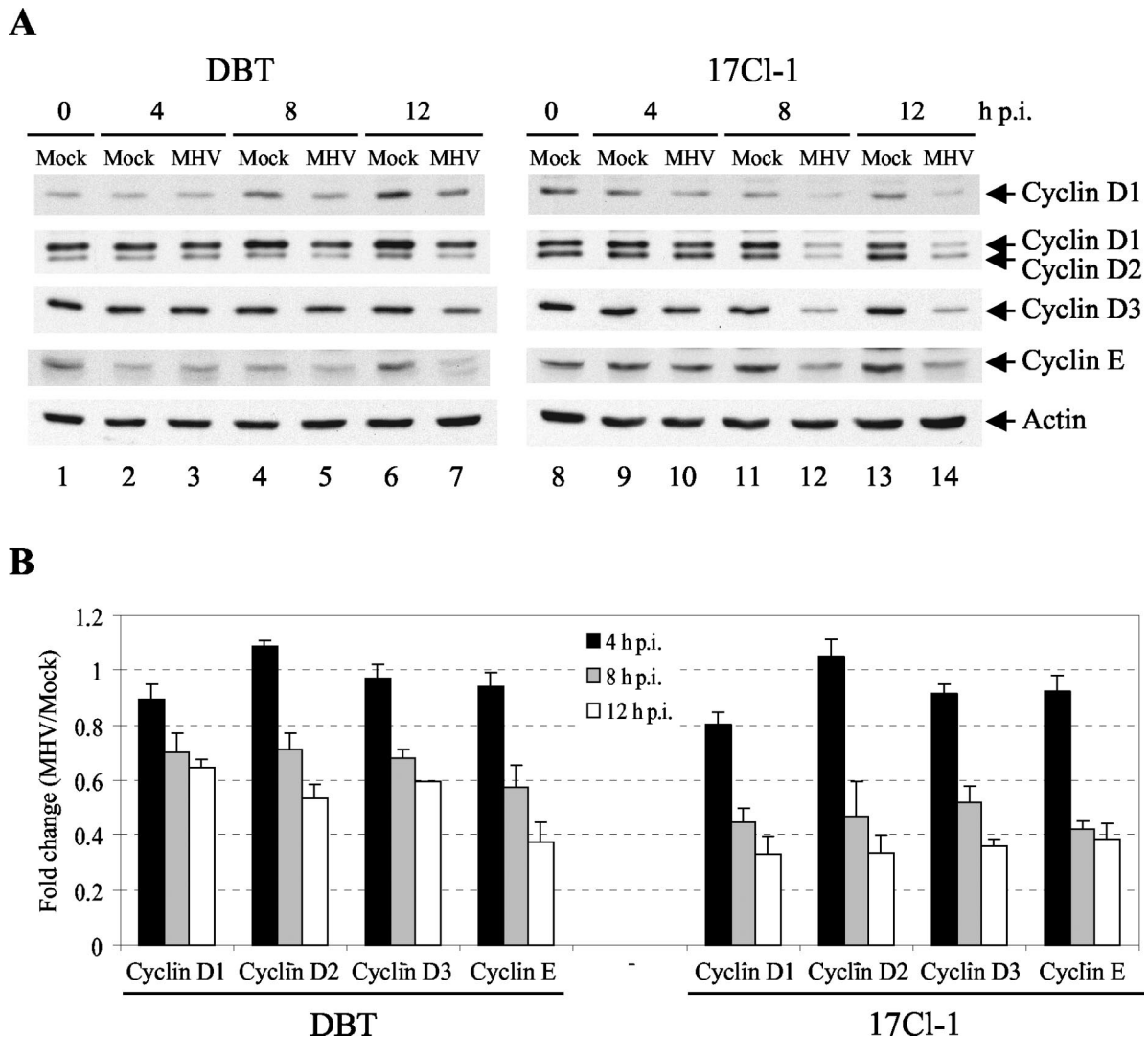
FIG. 8. Effect of MHV infection on levels of G_1 cyclins in asynchronously growing cells. (A) DBT and 17Cl-1 cells were mock infected (Mock) or infected with MHV-2 (MHV) at an MOI of 10. At the indicated times p.i., cells were lysed with SDS sample buffer, and equal amounts of protein from the samples were tested by Western blot analysis against probes for cyclin D1, cyclin D2, cyclin D3, cyclin E, and actin. The data are from one of three independent experiments. (B) Cyclin amounts in panel A were quantified by densitometric analysis and normalized against an internal control (actin). Bars indicate the ratio of cyclin amounts in MHV-infected samples to those in mock-infected samples. The results are presented as means and SEs ($n = 3$).

and E were all markedly smaller in MHV-infected cells than in mock-infected cells of both types at 8 and 12 h p.i. (Fig. 8). Our results suggested that the reduction in Cdk2 activity (Fig. 5) was most likely due to the decreases in the amounts of cyclin E and phospho-Cdk2 in MHV-infected cells, and we speculate that decreases in the levels of Cdk4/6 and D-type cyclins might result in reduced Cdk4/6 activities. Decreases in these Cdk activities would lead to the accumulation of nonphosphorylated and/or hypophosphorylated pRb and the arrest of the cell cycle in the G_0/G_1 phase.

To further establish the correlation between G_1 cyclin-Cdk levels and MHV-induced cell cycle arrest, we examined the amounts of G_1 cyclins and Cdks in MHV-infected quiescent 17Cl-1 cells after serum stimulation. Cyclin and Cdk levels

were determined by Western blot analysis (Fig. 9A) and quantified by scanning densitometry (Fig. 9B). Serum-starved quiescent cells had smaller amounts of Cdk4, Cdk6, cyclin D1, and cyclin D3, all of which were expressed in larger amounts after mitogenic stimulation in mock-infected cells (Fig. 9). In MHV-infected cells, on the other hand, the expression of Cdk4, Cdk6, cyclin D1, and cyclin D3 remained at a relatively low level after serum stimulation (Fig. 9). The amounts of cyclin D2 and cyclin E were not significantly increased at 15 and 18 h p.i. in mock-infected cells, whereas decreases in the amounts of both cyclins occurred in MHV-infected cells (Fig. 9). In summary, our data suggested that MHV infection resulted in decreases in the amounts of G_1 cyclin-Cdk complexes which led to reduced Cdk activities,

A
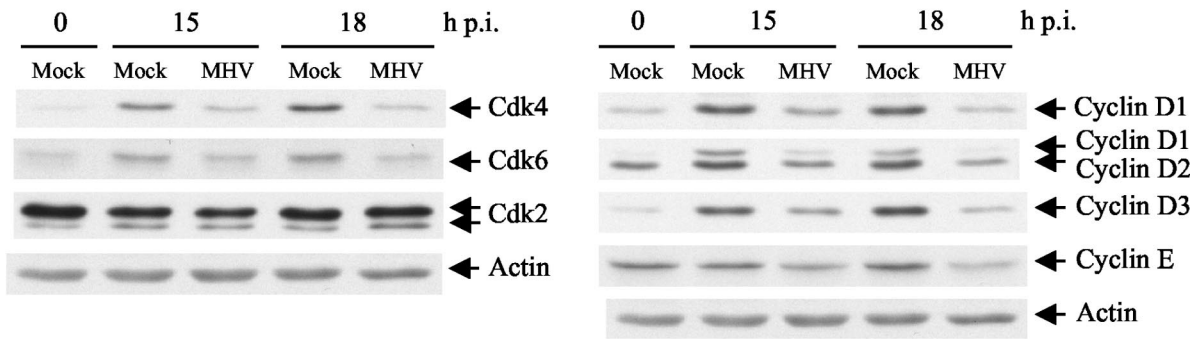
B
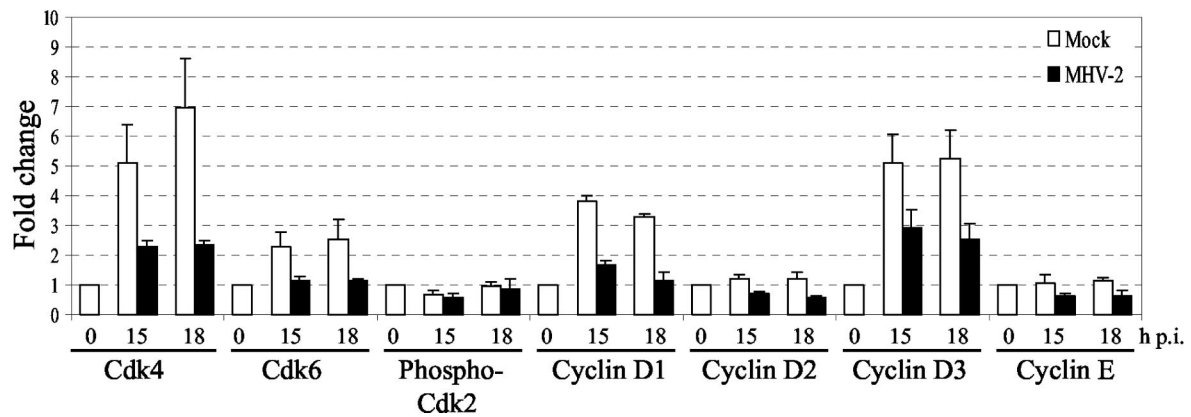
FIG. 9. Effect of MHV infection on levels of G_1 Cdks and G_1 cyclins in cells released from quiescence. (A) Serum-starved 17Cl-1 cells were mock infected (Mock) or infected with MHV-2 (MHV) at an MOI of 10. After 1 h of virus adsorption, medium containing 10% FCS was added to the cells. At the indicated times p.i., cells were lysed with SDS sample buffer, and equal amounts of protein from the samples were tested by Western blot analysis against probes for Cdk2, Cdk4, Cdk6, cyclin D1, cyclin D2, cyclin D3, cyclin E, and actin. The data are from one of three independent experiments. (B) Cdk and cyclin amounts in panel A were quantified by densitometric analysis and normalized against an internal control (actin). The amounts of each Cdk and each cyclin at different times p.i. were further normalized to the amounts at 0 h p.i., which were arbitrarily set to a value of 1.0. The results are presented as means and SEs ($n = 3$).

inefficient pRb hyperphosphorylation, and the accumulation of infected cells in the G_0/G_1 phase of the cell cycle (Fig. 10).

DISCUSSION

In this study, we investigated the effect of MHV infection on host cell cycle progression. Analysis of [^{3}H]thymidine incorporation demonstrated that MHV infection resulted in the inhibition of cellular DNA synthesis, and this effect required active MHV replication. FACS analyses demonstrated that MHV infection in actively growing cells caused an increase in the percentage of cells in the G_0/G_1 phase and that MHV infection in quiescent G_0-phase cells significantly prevented the cells from entering the S phase after mitogenic stimulation. Consistent with the cell cycle profile data, MHV replication inhibited pRb hyperphosphorylation, which is an essential step for E2F activation and S-phase progression. All of these data indicated that MHV replication arrested cell cycle progression in the
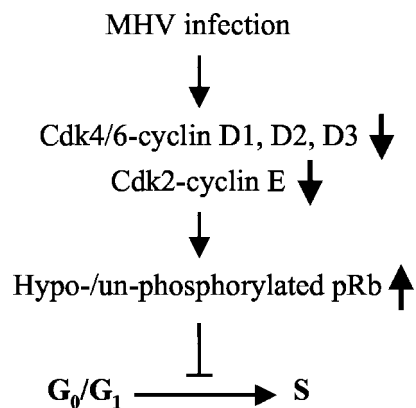
FIG. 10. Proposed mechanism for MHV-induced G_0/G_1 cell cycle arrest. MHV infection causes decreases in the amounts of G_1 cyclins and Cdks, resulting in a reduction in Cdk2/4/6 activities and the accumulation of hypophosphorylated and/or nonphosphorylated pRb, which blocks cell cycle progression from the G_0/G_1 phase to the S phase.

G_0/G_1 phase. A decrease in Cdk2 kinase activity was seen in MHV-infected DBT and 17Cl-1 cells, while the amounts of the CKIs p21^{Cip1}, p27^{Kip1}, and p16^{INK4a} did not change in infected cells. These data indicated that MHV-induced inhibition of Cdk2 activity (Fig. 5) and pRb hyperphosphorylation (Fig. 4) was not caused by the activation of these CKIs. MHV replication in asynchronous cultures, however, resulted in reduced amounts of G_1 cyclins in both DBT and 17Cl-1 cells as well as in decreases in Cdk4 and Cdk6 levels in 17Cl-1 cells. When quiescent 17Cl-1 cells were infected with MHV, they failed to accumulate Cdk4, Cdk6, cyclin D1, and cyclin D3 after serum stimulation, contrary to the increased accumulation of these G_1 cyclins and Cdks in mock-infected cells. In mock-infected cells, the levels of cyclins D2 and E remained unchanged at 18 h p.i. (17 h after serum stimulation), while MHV infection induced a reduction in the levels of these two cyclins. A straightforward interpretation of all of these data is that the formation of only limited amounts of G_1 cyclin-Cdk complexes led to reduced Cdk activities and insufficient pRb hyperphosphorylation, resulting in an inhibition or delay of cell cycle progression in the G_0/G_1 phase in MHV-infected cells. Because most of our biochemical studies were focused on proteins that are known to be involved in cell cycle progression in the G_0/G_1 phase, our studies did not rule out the possibility that MHV replication also affected other stages of the cell cycle progression. Further studies are required to characterize the effect of MHV replication on other cell cycle stages.

We have not determined exactly which point of progression in the cell cycle becomes inhibited in the G_0/G_1 phase of MHV-infected cells, but we can speculate on where the host cell cycle is arrested based on our analyses of various G_1 regulatory proteins. Actively growing cells go through repeated cycles of the $G_1/S/G_2/M$ phases, and when the environment is deprived of growth factors, cells enter the quiescent G_0 phase. The majority of uninfected cells showing 2N DNA content in FACS analysis therefore probably represented G_1 cells in actively growing cultures (Fig. 2A) and G_0 cells in serum-starved cultures (Fig. 3A). In the G_0 phase, pRb is nonphosphorylated; then it is sequentially hypophosphorylated by cyclin D-Cdk4/6 complexes in early G_1 and hyperphosphorylated by the cyclin E-Cdk2 complex in late G_1 (47). The loss of hyperphosphorylated pRb (Fig. 4A and B) and the reduction in Cdk2 activity (Fig. 5) after MHV infection in cycling cells indicated that infected cells failed to enter the late G_1 phase. The reduction in the amounts of Cdk4, Cdk6, and D-type cyclins (Fig. 7 and 8) in MHV-infected cells most likely caused the suppression of Cdk4/6 activities. Taken together, these results indicate that MHV-infected cells were most likely arrested in the early G_1 phase. MHV infection of 17Cl-1 cells synchronized in the G_0 phase resulted in a very limited increase in the amounts of Cdk4, Cdk6, and cyclins D1 and D3 and a decrease in the amount of cyclin D2 after serum stimulation (Fig. 9), indicating very low Cdk4/6 activities in these cells. Accordingly, cell cycle progression from G_0 to G_1 was most likely blocked in cells synchronized in the G_0 phase, and the cells probably remained in a G_0-like state. A previous report on measles virus-induced cell cycle arrest in T cells examined the amount of rRNA as a method for discrimination between G_0 cells with fewer ribosomes and G_1 cells with a higher level of ribosomes (53). Unfortunately, this experimental approach was not suit-

able for determining the exact point of MHV-induced cell cycle arrest, because MHV replication induces severe 28S rRNA degradation (3).

MHV replication caused a reduction in the amounts of G_1 cyclins (Fig. 8 and 9). The lower level of cyclin E might have resulted in reduced cyclin E-Cdk2 activity, and the lower levels of D-type cyclins most likely resulted in reduced cyclin D-Cdk4/6 activities. What, then, is the mechanism of reduction of the amounts of G_1 cyclins in MHV-infected cells? Because the amounts of cyclins can be regulated by their synthesis and degradation, MHV replication could affect G_1 cyclin levels through both mechanisms. DNA microarray analyses with several MHV-permissive cell lines revealed a slight decrease in cyclin D1 mRNA levels in MHV-infected cells (C. J. Chen and S. Makino, unpublished data), suggesting that MHV infection could affect cyclin mRNA transcriptional activity or stability. MHV replication might also affect cyclin translation, because host protein synthesis is suppressed in MHV-infected cells (3, 33, 66, 70, 71). Furthermore, MHV infection may promote cyclin D2 and E degradation; the amounts of cyclins D2 and E increased slightly after serum stimulation in quiescent 17Cl-1 cells but decreased after MHV infection in quiescent 17Cl-1 cells (Fig. 9). Decreased expression of cyclins and Cdks appears to be a common mechanism by which several viruses disrupt G_1 cell cycle progression, as demonstrated for the cell cycle arrest induced by herpes simplex virus type 1 (19, 67), coxsackievirus (48), and measles virus (53). For coxsackievirus, virus replication induces cell cycle arrest in part through an increase in the ubiquitin-dependent proteolysis of cyclin D1 (48).

The expression of transmissible gastroenteritis virus N protein results in a higher percentage of cells undergoing cell division, suggesting a cell cycle delay or arrest in the G_2/M phase (81). Disrupted cytokinesis is also observed in cells expressing IBV N protein and cells infected with IBV (8). We did not detect an increase in the G_2/M-phase population in MHV-infected asynchronous cultures (Fig. 2), indicating that MHV N protein does not have an effect on cytokinesis or that its putative effect on cytokinesis is masked by other MHV-induced functions in infected cells.

What is the biological significance of MHV-induced cell cycle arrest? One possibility is that cell cycle arrest in the G_0/G_1 phase provides increased amounts of ribonucleotide pools for efficient MHV RNA synthesis; ribonucleotides are the precursors for synthesizing deoxyribonucleotides, and a reduction in cellular DNA synthesis most likely increases the levels of ribonucleotide pools in cells. Cell cycle arrest may also benefit MHV replication in some other ways. MHV replication in cultured cells generally results in cell death, including apoptotic cell death (2, 4, 7). The onset of caspase activation and apoptosis occurs very late p.i., when the highest level of MHV production has been achieved (7), yet how MHV manages to accomplish its maximum replication prior to cell death is unknown. Accumulated data from other laboratories imply that cross talk exists between cell cycle signaling and apoptosis signaling; apoptosis follows cell cycle arrest in some systems (28, 68), but in others, the induction of apoptosis appears to require progression through the cell cycle (83). It is possible that cell cycle arrest in MHV-infected cells prevents the induction and execution of early cell death in infected cells. Cell

cycle arrest may also assist in efficient MHV assembly, which occurs in the intermediate compartment between the endoplasmic reticulum and the Golgi complex (40, 74) and most likely requires proper intracellular membrane structures, whereas most membrane trafficking steps are disrupted during mitosis (46, 76). Indeed, a one-step growth curve for MHV-2 in DBT cells shows that exponential virus production occurs from 4 to 10 h p.i. and that the highest virus titer is maintained from 12 to 24 h p.i (35); the most efficient virus production occurs when infected cells are arrested in the G_0/G_1 phase, indicating that the MHV-induced cell cycle arrest may assist in efficient MHV assembly. Furthermore, cell cycle arrest may be beneficial to MHV protein synthesis. Cap-dependent translation is reduced during mitosis due to the impaired function of cap-binding protein (5). Because all MHV mRNAs are 5′ capped and the translation of all MHV proteins, except for E protein (73), is cap dependent, arresting cells in the G_0/G_1 phase to prevent cells from entering mitosis should be beneficial for the cap-dependent translation of MHV proteins. Finally, MHV-induced cell cycle arrest potentially has additional important biological significance for virus-induced pathogenicity. It has been reported that noncycling cells are less likely to be killed by cytotoxic T cells (54); hence, MHV-infected cells that are arrested in the G_0/G_1 phase may not be killed efficiently by cytotoxic T cells.

ACKNOWLEDGMENT

REFERENCES

1. **Aktas, H., H. Cai, and G. M. Cooper.** 1997. Ras links growth factor signaling to the cell cycle machinery via regulation of cyclin D1 and the Cdk inhibitor p27[KIP1]. Mol. Cell. Biol. **17:**3850–3857.
2. **An, S., C. J. Chen, X. Yu, J. L. Leibowitz, and S. Makino.** 1999. Induction of apoptosis in murine coronavirus-infected cultured cells and demonstration of E protein as an apoptosis inducer. J. Virol. **73:**7853–7859.
3. **Banerjee, S., S. An, A. Zhou, R. H. Silverman, and S. Makino.** 2000. RNase L-independent specific 28S rRNA cleavage in murine coronavirus-infected cells. J. Virol. **74:**8793–8802.
4. **Belyavsky, M., E. Belyavskaya, G. A. Levy, and J. L. Leibowitz.** 1998. Coronavirus MHV-3-induced apoptosis in macrophages. Virology **250:**41–49.
5. **Bonneau, A. M., and N. Sonenberg.** 1987. Involvement of the 24-kDa cap-binding protein in regulation of protein synthesis in mitosis. J. Biol. Chem. **262:**11134–11139.
6. **Botz, J., K. Zerfass-Thome, D. Spitkovsky, H. Delius, B. Vogt, M. Eilers, A. Hatzigeorgiou, and P. Jansen-Durr.** 1996. Cell cycle regulation of the murine cyclin E gene depends on an E2F binding site in the promoter. Mol. Cell. Biol. **16:**3401–3409.
7. **Chen, C. J., and S. Makino.** 2002. Murine coronavirus-induced apoptosis in 17Cl-1 cells involves a mitochondria-mediated pathway and its downstream caspase-8 activation and bid cleavage. Virology **302:**321–332.
8. **Chen, H., T. Wurm, P. Britton, G. Brooks, and J. A. Hiscox.** 2002. Interaction of the coronavirus nucleoprotein with nucleolar antigens and the host cell. J. Virol. **76:**5233–5250.
9. **Clurman, B. E., R. J. Sheaff, K. Thress, M. Groudine, and J. M. Roberts.** 1996. Turnover of cyclin E by the ubiquitin-proteasome pathway is regulated by cdk2 binding and cyclin phosphorylation. Genes Dev. **10:**1979–1990.
10. **Compton, S. R., S. W. Barthold, and A. L. Smith.** 1993. The cellular and molecular pathogenesis of coronaviruses. Lab. Anim. Sci. **43:**15–28.
11. **Connell-Crowley, L., J. W. Harper, and D. W. Goodrich.** 1997. Cyclin D1/Cdk4 regulates retinoblastoma protein-mediated cell cycle arrest by site-specific phosphorylation. Mol. Biol. Cell **8:**287–301.
12. **Cox, D. C., and J. E. Shaw.** 1974. Inhibition of the initiation of cellular DNA synthesis after reovirus infection. J. Virol. **13:**760–761.
13. **DeCaprio, J. A., J. W. Ludlow, J. Figge, J. Y. Shew, C. M. Huang, W. H. Lee, E. Marsilio, E. Paucha, and D. M. Livingston.** 1988. SV40 large tumor antigen forms a specific complex with the product of the retinoblastoma susceptibility gene. Cell **54:**275–283.
14. **DeCaprio, J. A., J. W. Ludlow, D. Lynch, Y. Furukawa, J. Griffin, H. Piwnica-Worms, C. M. Huang, and D. M. Livingston.** 1989. The product of the retinoblastoma susceptibility gene has properties of a cell cycle regulatory element. Cell **58:**1085–1095.
15. **Diehl, J. A., M. Cheng, M. F. Roussel, and C. J. Sherr.** 1998. Glycogen synthase kinase-3beta regulates cyclin D1 proteolysis and subcellular localization. Genes Dev. **12:**3499–3511.
16. **Drosten, C., S. Gunther, W. Preiser, S. van der Werf, H. R. Brodt, S. Becker, H. Rabenau, M. Panning, L. Kolesnikova, R. A. Fouchier, A. Berger, A. M. Burguiere, J. Cinatl, M. Eickmann, N. Escriou, K. Grywna, S. Kramme, J. C. Manuguerra, S. Muller, V. Rickerts, M. Sturmer, S. Vieth, H. D. Klenk, A. D. Osterhaus, H. Schmitz, and H. W. Doerr.** 2003. Identification of a novel coronavirus in patients with severe acute respiratory syndrome. N. Engl. J. Med. **348:**1967–1976.
17. **Dyson, N.** 1998. The regulation of E2F by pRB-family proteins. Genes Dev. **12:**2245–2262.
18. **Eckner, R., M. E. Ewen, D. Newsome, M. Gerdes, J. A. DeCaprio, J. B. Lawrence, and D. M. Livingston.** 1994. Molecular cloning and functional analysis of the adenovirus E1A-associated 300-kD protein (p300) reveals a protein with properties of a transcriptional adaptor. Genes Dev. **8:**869–884.
19. **Ehmann, G. L., T. I. McLean, and S. L. Bachenheimer.** 2000. Herpes simplex virus type 1 infection imposes a G_1/S block in asynchronously growing cells and prevents G_1 entry in quiescent cells. Virology **267:**335–349.
20. **Ensminger, W. D., and I. Tamm.** 1969. The step in cellular DNA synthesis blocked by reovirus infection. Virology **39:**935–938.
21. **Ezhevsky, S. A., H. Nagahara, A. M. Vocero-Akbani, D. R. Gius, M. C. Wei, and S. F. Dowdy.** 1997. Hypo-phosphorylation of the retinoblastoma protein (pRb) by cyclin D:Cdk4/6 complexes results in active pRb. Proc. Natl. Acad. Sci. USA **94:**10699–10704.
22. **Fanning, E., and R. Knippers.** 1992. Structure and function of simian virus 40 large tumor antigen. Annu. Rev. Biochem. **61:**55–85.
23. **Fesquet, D., J. C. Labbe, J. Derancourt, J. P. Capony, S. Galas, F. Girard, T. Lorca, J. Shuttleworth, M. Doree, and J. C. Cavadore.** 1993. The MO15 gene encodes the catalytic subunit of a protein kinase that activates cdc2 and other cyclin-dependent kinases (CDKs) through phosphorylation of Thr161 and its homologues. EMBO J. **12:**3111–3121.
24. **Filmus, J., A. I. Robles, W. Shi, M. J. Wong, L. L. Colombo, and C. J. Conti.** 1994. Induction of cyclin D1 overexpression by activated ras. Oncogene **9:**3627–3633.
25. **Flemington, E. K.** 2001. Herpesvirus lytic replication and the cell cycle: arresting new developments. J. Virol. **75:**4475–4481.
26. **Geng, Y., E. N. Eaton, M. Picon, J. M. Roberts, A. S. Lundberg, A. Gifford, C. Sardet, and R. A. Weinberg.** 1996. Regulation of cyclin E transcription by E2Fs and retinoblastoma protein. Oncogene **12:**1173–1180.
27. **Goh, W. C., M. E. Rogel, C. M. Kinsey, S. F. Michael, P. N. Fultz, M. A. Nowak, B. H. Hahn, and M. Emerman.** 1998. HIV-1 Vpr increases viral expression by manipulation of the cell cycle: a mechanism for selection of Vpr in vivo. Nat. Med. **4:**65–71.
28. **Gozlan, J., J. L. Lathey, and S. A. Spector.** 1998. Human immunodeficiency virus type 1 induction mediated by genistein is linked to cell cycle arrest in G_2. J. Virol. **72:**8174–8180.
29. **Gu, Y., J. Rosenblatt, and D. O. Morgan.** 1992. Cell cycle regulation of CDK2 activity by phosphorylation of Thr160 and Tyr15. EMBO J. **11:**3995–4005.
30. **Hand, R., W. D. Ensminger, and I. Tamm.** 1971. Cellular DNA replication in infections with cytocidal RNA viruses. Virology **44:**527–536.
31. **Harbour, J. W., and D. C. Dean.** 2000. The Rb/E2F pathway: expanding roles and emerging paradigms. Genes Dev. **14:**2393–2409.
32. **He, J., S. Choe, R. Walker, P. Di Marzio, D. O. Morgan, and N. R. Landau.** 1995. Human immunodeficiency virus type 1 viral protein R (Vpr) arrests cells in the G_2 phase of the cell cycle by inhibiting p34[cdc2] activity. J. Virol. **69:**6705–6711.
33. **Hilton, A., L. Mizzen, G. MacIntyre, S. Cheley, and R. Anderson.** 1986. Translational control in murine hepatitis virus infection. J. Gen. Virol. **67:**923–932.
34. **Hirano, N., K. Fujiwara, S. Hino, and M. Matsumoto.** 1974. Replication and plaque formation of mouse hepatitis virus (MHV-2) in mouse cell line DBT culture. Arch. Gesamte Virusforch. **44:**298–302.
35. **Hirano, N., K. Fujiwara, and M. Matumoto.** 1976. Mouse hepatitis virus (MHV-2). Plaque assay and propagation in mouse cell line DBT cells. Jpn. J. Microbiol. **20:**219–225.
36. **Howe, J. A., J. S. Mymryk, C. Egan, P. E. Branton, and S. T. Bayley.** 1990. Retinoblastoma growth suppressor and a 300-kDa protein appear to regulate cellular DNA synthesis. Proc. Natl. Acad. Sci. USA **87:**5883–5887.
37. **Keck, J. G., L. H. Soe, S. Makino, S. A. Stohlman, and M. M. Lai.** 1988. RNA recombination of murine coronaviruses: recombination between fusion-positive mouse hepatitis virus A59 and fusion-negative mouse hepatitis virus 2. J. Virol. **62:**1989–1998.
38. **Kerkhoff, E., and U. R. Rapp.** 1997. Induction of cell proliferation in quiescent NIH 3T3 cells by oncogenic c-Raf-1. Mol. Cell. Biol. **17:**2576–2586.
39. **Kitagawa, M., H. Higashi, H. K. Jung, I. Suzuki-Takahashi, M. Ikeda, K. Tamai, J. Kato, K. Segawa, E. Yoshida, S. Nishimura, and Y. Taya.** 1996. The consensus motif for phosphorylation by cyclin D1-Cdk4 is different from that for phosphorylation by cyclin A/E-Cdk2. EMBO J. **15:**7060–7069.

40. Klumperman, J., J. K. Locker, A. Meijer, M. C. Horzinek, H. J. Geuze, and P. J. Rottier. 1994. Coronavirus M proteins accumulate in the Golgi complex beyond the site of virion budding. J. Virol. 68:6523–6534.

41. Knudsen, E. S., and J. Y. Wang. 1996. Differential regulation of retinoblastoma protein function by specific Cdk phosphorylation sites. J. Biol. Chem. 271:8313–8320.

42. Ksiazek, T. G., D. Erdman, C. S. Goldsmith, S. R. Zaki, T. Peret, S. Emery, S. Tong, C. Urbani, J. A. Comer, W. Lim, P. E. Rollin, S. F. Dowell, A. E. Ling, C. D. Humphrey, W. J. Shieh, J. Guarner, C. D. Paddock, P. Rota, B. Fields, J. DeRisi, J. Y. Yang, N. Cox, J. M. Hughes, J. W. LeDuc, W. J. Bellini, and L. J. Anderson. 2003. A novel coronavirus associated with severe acute respiratory syndrome. N. Engl. J. Med. 348:1953–1966.

43. Lavoie, J. N., G. L'Allemain, A. Brunet, R. Muller, and J. Pouyssegur. 1996. Cyclin D1 expression is regulated positively by the p42/p44MAPK and negatively by the p38/HOGMAPK pathway. J. Biol. Chem. 271:20608–20616.

44. Lin, G. Y., and R. A. Lamb. 2000. The paramyxovirus simian virus 5 V protein slows progression of the cell cycle. J. Virol. 74:9152–9166.

45. Locker, J. K., J. Klumperman, V. Oorschot, M. C. Horzinek, H. J. Geuze, and P. J. Rottier. 1994. The cytoplasmic tail of mouse hepatitis virus M protein is essential but not sufficient for its retention in the Golgi complex. J. Biol. Chem. 269:28263–28269.

46. Lowe, M., N. Nakamura, and G. Warren. 1998. Golgi division and membrane traffic. Trends Cell Biol. 8:40–44.

47. Lundberg, A. S., and R. A. Weinberg. 1998. Functional inactivation of the retinoblastoma protein requires sequential modification by at least two distinct cyclin-cdk complexes. Mol. Cell. Biol. 18:753–761.

48. Luo, H., J. Zhang, F. Dastvan, B. Yanagawa, M. A. Reidy, H. M. Zhang, D. Yang, J. E. Wilson, and B. M. McManus. 2003. Ubiquitin-dependent proteolysis of cyclin D1 is associated with coxsackievirus-induced cell growth arrest. J. Virol. 77:1–9.

49. McChesney, M. B., A. Altman, and M. B. Oldstone. 1988. Suppression of T lymphocyte function by measles virus is due to cell cycle arrest in G1. J. Immunol. 140:1269–1273.

50. McChesney, M. B., J. H. Kehrl, A. Valsamakis, A. S. Fauci, and M. B. Oldstone. 1987. Measles virus infection of B lymphocytes permits cellular activation but blocks progression through the cell cycle. J. Virol. 61:3441–3447.

51. Nakayama, K. 1998. Cip/Kip cyclin-dependent kinase inhibitors: brakes of the cell cycle engine during development. Bioessays 20:1020–1029.

52. Nakayama, K., H. Nagahama, Y. A. Minamishima, M. Matsumoto, I. Nakamichi, K. Kitagawa, M. Shirane, R. Tsunematsu, T. Tsukiyama, N. Ishida, M. Kitagawa, and S. Hatakeyama. 2000. Targeted disruption of Skp2 results in accumulation of cyclin E and p27Kip1, polyploidy and centrosome overduplication. EMBO J. 19:2069–2081.

53. Naniche, D., S. I. Reed, and M. B. Oldstone. 1999. Cell cycle arrest during measles virus infection: a G0-like block leads to suppression of retinoblastoma protein expression. J. Virol. 73:1894–1901.

54. Nishioka, W. K., and R. M. Welsh. 1994. Susceptibility to cytotoxic T lymphocyte-induced apoptosis is a function of the proliferative status of the target. J. Exp. Med. 179:769–774.

55. Obaya, A. J., and J. M. Sedivy. 2002. Regulation of cyclin-Cdk activity in mammalian cells. Cell. Mol. Life Sci. 59:126–142.

56. Op De Beeck, A., and P. Caillet-Fauquet. 1997. Viruses and the cell cycle. Prog. Cell Cycle Res. 3:1–19.

57. Perlman, S. 1998. Pathogenesis of coronavirus-induced infections. Review of pathological and immunological aspects. Adv. Exp. Med. Biol. 440:503–513.

58. Pines, J. 1993. Cyclins and cyclin-dependent kinases: take your partners. Trends Biochem. Sci. 18:195–197.

59. Poggioli, G. J., C. Keefer, J. L. Connolly, T. S. Dermody, and K. L. Tyler. 2000. Reovirus-induced G2/M cell cycle arrest requires σ1s and occurs in the absence of apoptosis. J. Virol. 74:9562–9570.

60. Re, F., D. Braaten, E. K. Franke, and J. Luban. 1995. Human immunodeficiency virus type 1 Vpr arrests the cell cycle in G2 by inhibiting the activation of p34cdc2-cyclin B. J. Virol. 69:6859–6864.

61. Reshetnikova, G., R. Barkan, B. Popov, N. Nikolsky, and L. S. Chang. 2000. Disruption of the actin cytoskeleton leads to inhibition of mitogen-induced cyclin E expression, Cdk2 phosphorylation, and nuclear accumulation of the retinoblastoma protein-related p107 protein. Exp. Cell Res. 259:35–53.

62. Rogel, M. E., L. I. Wu, and M. Emerman. 1995. The human immunodeficiency virus type 1 vpr gene prevents cell proliferation during chronic infection. J. Virol. 69:882–888.

63. Roussel, M. F. 1999. The INK4 family of cell cycle inhibitors in cancer. Oncogene 18:5311–5317.

64. Shapiro, G. I., C. D. Edwards, and B. J. Rollins. 2000. The physiology of p16INK4A-mediated G1 proliferative arrest. Cell Biochem. Biophys. 33:189–197.

65. Sherr, C. J., and J. M. Roberts. 1999. CDK inhibitors: positive and negative regulators of G1-phase progression. Genes Dev. 13:1501–1512.

66. Siddell, S., H. Wege, A. Barthel, and V. ter Meulen. 1981. Coronavirus JHM: intracellular protein synthesis. J. Gen. Virol. 53:145–155.

67. Song, B., J. J. Liu, K. C. Yeh, and D. M. Knipe. 2000. Herpes simplex virus infection blocks events in the G1 phase of the cell cycle. Virology 267:326–334.

68. Stewart, S. A., B. Poon, J. B. Jowett, Y. Xie, and I. S. Chen. 1999. Lentiviral delivery of HIV-1 Vpr protein induces apoptosis in transformed cells. Proc. Natl. Acad. Sci. USA 96:12039–12043.

69. Sturman, L. S., and K. K. Takemoto. 1972. Enhanced growth of a murine coronavirus in transformed mouse cells. Infect. Immun. 6:501–507.

70. Tahara, S., C. Bergmann, G. Nelson, R. Anthony, T. Dietlin, S. Kyuwa, and S. Stohlman. 1993. Effects of mouse hepatitis virus infection on host cell metabolism. Adv. Exp. Med. Biol. 342:111–116.

71. Tahara, S. M., T. A. Dietlin, C. C. Bergmann, G. W. Nelson, S. Kyuwa, R. P. Anthony, and S. A. Stohlman. 1994. Coronavirus translational regulation: leader affects mRNA efficiency. Virology 202:621–630.

72. Tamrakar, S., E. Rubin, and J. W. Ludlow. 2000. Role of pRB dephosphorylation in cell cycle regulation. Front. Biosci. 5:D121–D137.

73. Thiel, V., and S. G. Siddell. 1994. Internal ribosome entry in the coding region of murine hepatitis virus mRNA 5. J. Gen. Virol. 75:3041–3046.

74. Tooze, J., S. Tooze, and G. Warren. 1984. Replication of coronavirus MHV-A59 in sac− cells: determination of the first site of budding of progeny virions. Eur. J. Cell Biol. 33:281–293.

75. Vousden, K. H. 1994. Interactions between papillomavirus proteins and tumor suppressor gene products. Adv. Cancer Res. 64:1–24.

76. Warren, G. 1993. Membrane partitioning during cell division. Annu. Rev. Biochem. 62:323–348.

77. Weber, J. D., D. M. Raben, P. J. Phillips, and J. J. Baldassare. 1997. Sustained activation of extracellular-signal-regulated kinase 1 (ERK1) is required for the continued expression of cyclin D1 in G1 phase. Biochem. J. 326:61–68.

78. Wege, H., S. Siddell, and V. ter Meulen. 1982. The biology and pathogenesis of coronaviruses. Curr. Top. Microbiol. Immunol. 99:165–200.

79. Werness, B. A., A. J. Levine, and P. M. Howley. 1990. Association of human papillomavirus types 16 and 18 E6 proteins with p53. Science 248:76–79.

80. Won, K. A., and S. I. Reed. 1996. Activation of cyclin E/CDK2 is coupled to site-specific autophosphorylation and ubiquitin-dependent degradation of cyclin E. EMBO J. 15:4182–4193.

81. Wurm, T., H. Chen, T. Hodgson, P. Britton, G. Brooks, and J. A. Hiscox. 2001. Localization to the nucleolus is a common feature of coronavirus nucleoproteins, and the protein may disrupt host cell division. J. Virol. 75:9345–9356.

82. Yu, H., B. Bauer, G. K. Lipke, R. L. Phillips, and G. Van Zant. 1993. Apoptosis and hematopoiesis in murine fetal liver. Blood 81:373–384.

83. Zhu, L., and C. Anasetti. 1995. Cell cycle control of apoptosis in human leukemic T cells. J. Immunol. 154:192–200.